RSC Advances

PAPER

View Article Online
View Journal | View Issue

Cite this: *RSC Adv.*, 2017, **7**, 53861

Covalently anchored tertiary amine functionalized ionic liquid on silica coated nano-Fe_3O_4 as a novel, efficient and magnetically recoverable catalyst for the unsymmetrical Hantzsch reaction and Knoevenagel condensation†

Qiang Zhang, *[a] Xiao-Ming Ma,[b] Huai-Xin Wei,[a] Xin Zhao[a] and Jun Luo[c]

Received 27th September 2017
Accepted 15th November 2017

DOI: 10.1039/c7ra10692k

rsc.li/rsc-advances

A novel magnetic nanoparticle supported basic ionic liquid was successfully prepared by covalently anchoring 1-(2′-piperidyl)ethyl-3-(3-propyltriethoxysilane)imidazolium chloride onto the surface of silica-coated Fe_3O_4 nanoparticles, and characterized by FT-IR, TEM, XRD, TGA, VSM and elemental analysis. The obtained supported ionic liquid was certified as a versatile and robust catalyst for the unsymmetrical Hantzsch reaction and Knoevenagel condensation under solvent-free conditions. Furthermore, the catalyst could be conveniently recovered by an external magnet and reused six times without significant loss of catalytic activity.

Introduction

1,4-Dihydropyridines and polyhydroquinolines are important classes of bioactive molecules and heterocyclic scaffolds in pharmaceutical research.[1,2] For instance, nifedipine, nicardipine, amlodipine and felodipine, as well-known calcium antagonists, are often used for the treatment of angina pectoris and hypertension as well.[3] Moreover, the 1,4-dihydropyridine and polyhydroquinoline derivatives possess many other therapeutic and pharmacological properties such as antitumor,[4] antitubercular,[5] antidiabetic,[6] antibacterial,[7] potassium-channel opening,[8] acetylcholinesterase inhibition and neuroprotective agent.[9,10] Additionally, these compounds could effectively behave as organic hydride donors for asymmetric transfer hydrogenation.[11] Thus, the synthesis of 1,4-dihydropyridine and polyhydroquinoline derivatives is an interesting research challenge to synthetic chemists. A valuable method for the synthesis of 1,4-dihydropyridines was initially established by Arthur Hantzsch in 1881 *via* a multicomponent reaction of aldehydes with ethyl acetoacetate and ammonia.[12] Subsequently, a variety of improved methods for the synthesis of polyhydroquinolines, using metal triflates,[13,14] organocatalysts,[15] bakers' yeast,[16] CAN,[17] *p*-TSA,[18] FeF_3,[19] $Hf(NPf_2)_4$,[20] Ni or Pd nanoparticles,[21,22] KH_2PO_4,[23] microwave and ultrasound irradiation,[24,25] have been reported. However, these procedures suffer from one or more drawbacks in terms of using volatile organic solvents, long reaction time, low yields, tedious product separation and catalyst recycling. To overcome these limitations, some attractive heterogeneous catalysts such as In–SiO_2,[26] cellulose supported sulfamic acid,[27] ILOS@Fe/TSPP,[28] V–TiO_2,[29] SPPN polymer,[30] PdRuNi@GO,[31] boehmite-SSA,[32] nano-ZrO_2–SO_3H,[33] Fe_3O_4 supported Cu and Ni complex[34,35] are applied in this regard. Although these reported methods show respective advantages and provide better improvements for the synthesis of the target molecules, there is still scope for improvement, particularly towards developing a milder and cleaner protocol without using precious metals and organic solvents.

On the other hand, due to undetectable vapor pressure, high thermal stability, excellent solubility and catalytic activity, ionic liquids (ILs) have attracted considerable attention as green reaction media or catalysts.[36,37] Despite of their widespread use in organic reactions, some drawbacks, for instance difficult product separation and catalyst recovery due to their high viscosity, and use of large amounts of ILs in biphasic systems, still exist yet. More recently, a concept of nanoconfined ionic liquids has been proposed,[38] which combines the benefits of nano-supports and ILs, such as minimizing the dosage of ILs, high designability and excellent activity. However, nanoparticles are difficult to separate by filtration and expensive ultracentrifugation is the main way to separate the product and catalyst. This limitation can be overcame by using magnetic nanoparticles (MNPs), which can be simply recovered from the

[a]Jiangsu Key Laboratory of Environmental Functional Materials, School of Chemistry, Biology and Material Engineering, Suzhou University of Science and Technology, Suzhou 215009, China. E-mail: zhangqiang005@gmail.com

[b]School of Pharmaceutical Engineering & Life Science, Changzhou University, Changzhou 213164, China

[c]School of Chemical Engineering, Nanjing University of Science & Technology, Nanjing 210094, China

† Electronic supplementary information (ESI) available. See DOI: 10.1039/c7ra10692k

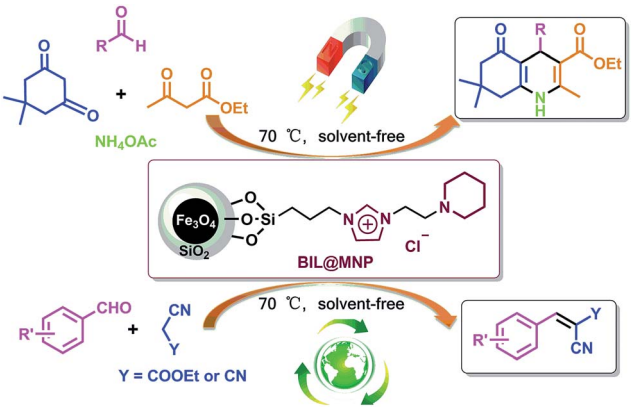

Scheme 1 The BIL@MNP catalyzed unsymmetrical Hantzsch reaction and Knoevenagel condensation.

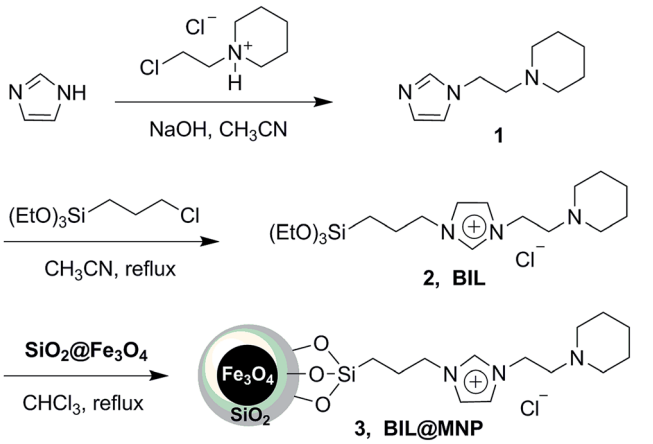

Scheme 2 The synthetic route for BIL@MNP.

reaction mixture by magnetic separation.[39] A variety of magnetically retrievable catalysts have been employed in a range of organic transformations,[40–42] and some immobilization processes for functional ILs on MNPs supports have been developed.[43–45]

In order to explore a new protocol for the synthesis of polyhydroquinolines and continue our investigations on the recoverable catalysts for organic transformations,[46–50] herein, we demonstrated a novel silica coated nano-Fe_3O_4 supported basic ionic liquid (BIL@MNP) and its application as a robust and magnetically recoverable catalyst for the one-pot synthesis of polyhydroquinolines *via* the unsymmetrical Hantzsch reaction. Interestingly, this novel catalyst could act as an efficient and reusable catalyst for Knoevenagel condensation under solvent-free conditions as well (Scheme 1).

Results and discussion

The magnetic nanoparticle supported basic ionic liquid catalyst (BIL@MNP) was prepared following the procedure shown in Scheme 2. *N*-(2-Chloroethyl)piperidine was firstly treated with imidazole to give 1-(2-(1*H*-imidazol-1-yl)ethyl)piperidine **1** under basic conditions. Then, a quaternization of (3-chloropropyl)triethoxysilane and the compound **1** afforded the precursor ionic liquid **2** (BIL). Ultimately, a suspension of SiO_2@Fe_3O_4 with a chloroform solution of the BIL was refluxed for 36 h to undergo a condensation reaction, which provided the desired catalyst **3** (BIL@MNP).

In order to confirm the successful functionalization of MNPs, FT-IR was employed to give a detailed investigation of the SiO_2@Fe_3O_4, BIL, and BIL@MNP (Fig. 1). The Si–O–Si and Fe–O vibrations of the SiO_2@Fe_3O_4 could be observed at around 1097 and 580 cm^{-1}, respectively. The IR curve of BIL shows typical bands at 1563 cm^{-1} (C=N vibration and C=C vibrations of the imidazole ring), 2941, 2866 and 1456 cm^{-1} (alkyl chain stretching and deformation vibrations). While in the spectrum of BIL@MNP, these characteristic peaks are at the similar wavenumbers, with a slight offset due to the interaction with the support. Nevertheless, all of these significant features cannot be observed in the support SiO_2@Fe_3O_4. Moreover, the nitrogen content of BIL@MNP determined by elemental analysis was 1.51%, which shows that the loading amount of the imino–pyridine ligand was calculated to be 0.36 mmol g^{-1}. The above results indicate that the BIL was successfully grafted onto the SiO_2@Fe_3O_4.

X-ray reflective diffraction (XRD) and transmission electron microscopy (TEM) were then carried out to obtain detailed information about the structure and morphology of as-prepared catalyst. The high-angle XRD pattern of BIL@MNP (Fig. 2) exhibits diffraction peaks corresponding to the standard Fe_3O_4 sample (JCPDS file no. 19-0629), which clearly indicates that the surface modification of MNPs do not damage the crystal structure of Fe_3O_4 core. And the TEM image of BIL@MNP shows that the dark nano-Fe_3O_4 cores are surrounded by grey silica shell and the average size of BIL@MNP is about 20 nm (Fig. 3a).

The stability of the BIL@MNP was determined by the thermogravimetric analysis (Fig. 4). The TG curve indicates an initial weight loss of 1.0% up to 150 °C due to the adsorbed

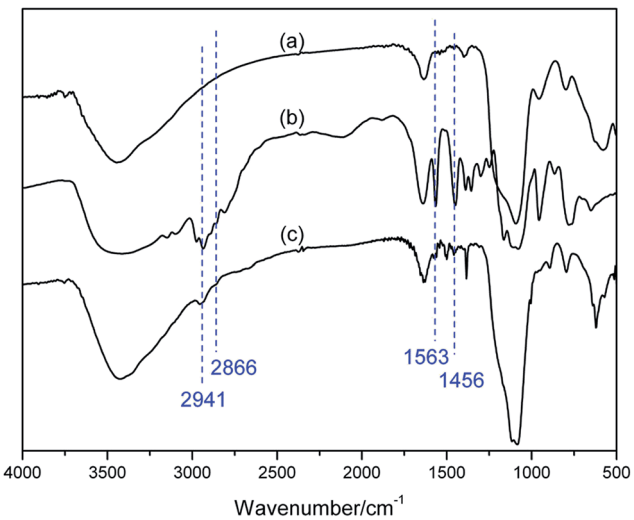

Fig. 1 FT-IR spectra of the SiO_2@Fe_3O_4 (a), BIL (b) and BIL@MNP (c).

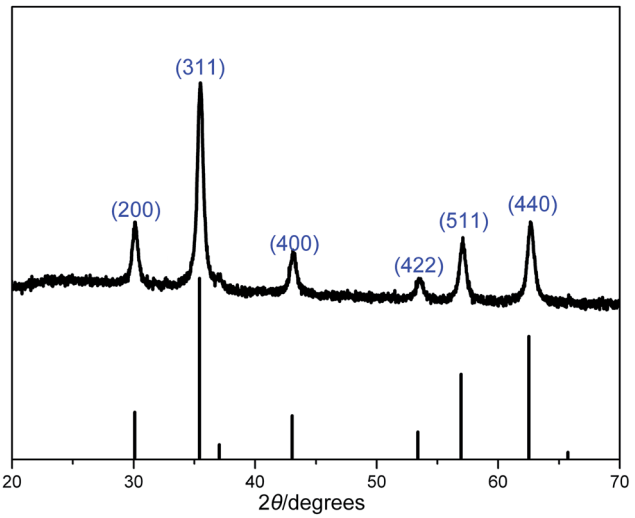

Fig. 2 XRD pattern of BIL@MNP. The bottom row of tick marks indicates the reflection positions for a standard magnetite pattern (JCPDS no. 19-0629).

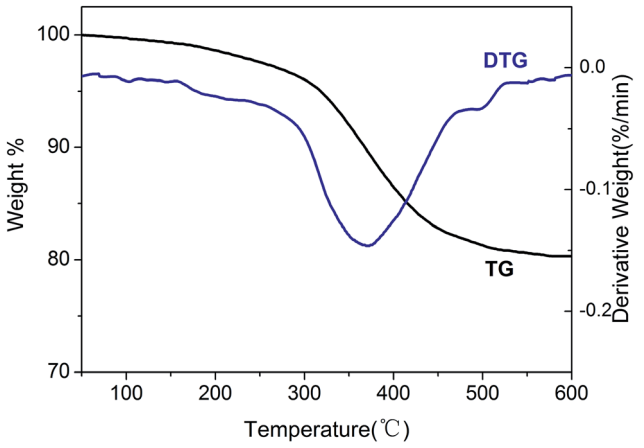

Fig. 4 TG-DTG analysis for AIL@MNP.

water in support. Complete loss of the supported IL was found in the temperature range from 200 °C to 500 °C, and the amount of organic structure was about 17.3% against the total solid catalyst. Meanwhile, the DTG curve shows that the decomposition of ionic moiety mainly occured in one step from 250 °C to 450 °C, which is related to main weight loss of 14.8%. And the peak in the DTG curve shows the fastest loss of the IL occured at 365 °C. Therefore, the BIL@MNP is stable below about 200 °C.

The magnetic property of BIL@MNP was evaluated using vibrating sample magnetometer (VSM) at room temperature. The VSM magnetization curve goes through the zero point (Fig. 5). The phenomenon of no magnetic hysteresis indicates that the as-prepared catalyst is superparamagnetic. As a result, BIL@MNP can be simply separated from the reaction mixture using an external magnet.

To investigate the catalytic activity of the newly designed catalyst, it was initially tested for the one-pot synthesis of polyhydroquinolines. The four-component condensation of benzaldehyde (1 mmol), dimedone (1 mmol), ethyl acetoacetate (1 mmol) and ammonium acetate (1 mmol), as a model reaction, was firstly performed in the presence of BIL@MNP (1.0 mol%) for 30 min at 70 °C under solvent-free conditions. And the corresponding product was obtained in 60% yield. Encouraged by this result, we increased gradually the amount of catalyst from 0 to 3.0 mol% (Table 1, entries 1–6). In the absence of BIL@MNP, only a small amount of product was detected, whereas the yield was improved as the amount of BIL@MNP increased from 0 to 2.5 mol% and became almost steady when the amount of catalyst was further increased beyond this. The influence of reaction temperature was also investigated (Table 1, entries 7–9), which indicated that lower temperatures (50–60 °C) decelerated the reaction rate and led to lower yields and no obvious improvement was achieved by the elevated temperature (80 °C). Hence, the best result was obtained in the presence of 2.5 mol% of BIL@MNP at 70 °C (Table 1, entry 5). In order to show the unique role of BIL@MNP, some control experiments in the presence of the SiO_2@Fe_3O_4 (blank support), BIL (unsupported ionic liquid) and triethylamine (traditional tertiary amine) were further carried out and they could also afford moderate to good yields under the same conditions (Table 1, entries 10–12). However, they were obviously inferior to the BIL@MNP. These results indicated that the high catalytic

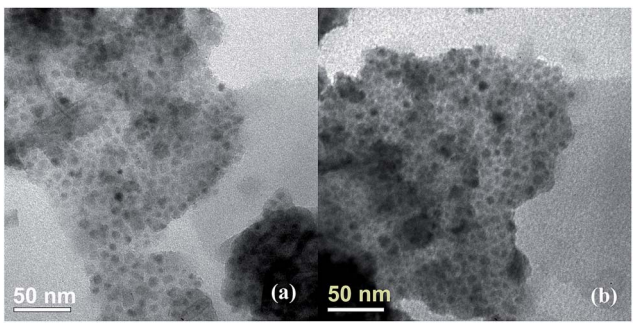

Fig. 3 TEM images of BIL@MNP (a) and six-times reused catalyst (b).

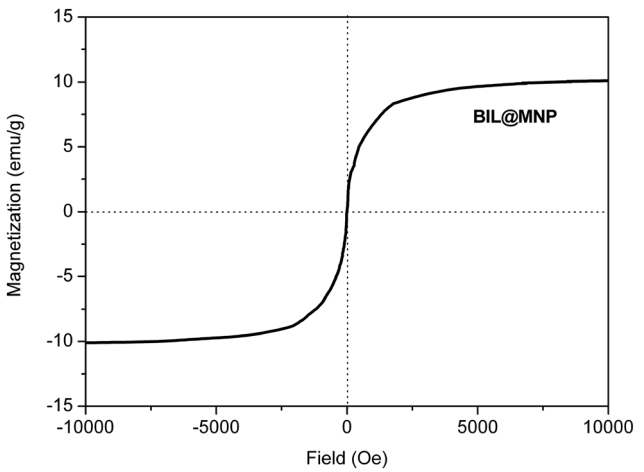

Fig. 5 Magnetic curve of BIL@MNP.

Table 1 Screening conditions for the model reaction

Entry	Catalyst (mol%)	Temperature (°C)	Time (min)	Isolated yield (%)
1	—	70	30	24
2	BIL@MNP (1.0)	70	30	60
3	BIL@MNP (1.5)	70	25	73
4	BIL@MNP (2.0)	70	20	84
5	**BIL@MNP (2.5)**	**70**	**15**	**92**
6	BIL@MNP (3.0)	70	15	92
7	BIL@MNP (2.5)	50	15	68
8	BIL@MNP (2.5)	60	15	85
9	BIL@MNP (2.5)	80	15	93
10	SiO_2@Fe_3O_4 (70 mg)	70	15	45
11	BIL (2.5)	70	15	81
12	NEt_3 (2.5)	70	15	70

activity of BIL@MNP for the one-pot synthesis of polyhydroquinolines could be attributed to the synergistic interaction between the surface silanol groups of nano-support and ionic liquid moieties.

The generality of this method for the four-component condensation of structurally diverse aldehydes, dimedone, ethyl acetoacetate and ammonium acetate under the optimized conditions was then investigated and the results are shown in Table 2. The aromatic aldehydes bearing either electron-withdrawing or electron-donating groups (Table 2, entries 1–13) were converted to the corresponding polyhydroquinolines in good to excellent yields (84–93%). Interestingly, heteroaromatic aldehydes such as thiophene-2-carbaldehyde and furan-2-carbaldehyde (Table 2, entries 14 and 15) also underwent these transformations well to afford the target products in excellent yields (86–90%). Furthermore, the aliphatic aldehyde, which is a usually less reactive substrate,[28] was smoothly converted to the corresponding product as well (Table 2, entry 16). These results demonstrate that the designed catalyst BIL@MNP showed an excellent performance for the one-pot synthesis of polyhydroquinolines.

In order to evaluate the merit of the method for the synthesis of polyhydroquinolines, we compared the efficiency of BIL@MNP with some recently reported catalysts for the one-pot four-component synthesis of **4a**. As shown in Table 3, BIL@MNP showed a better activity in terms of no precious metals, organic solvents or additional irradiation.

A plausible mechanism for the synthesis of polyhydroquinolines catalyzed by BIL@MNP is proposed in Scheme 3. Initially, the enol form of dimedone performs a nucleophilic addition to the activated aldehyde to provide the corresponding Knoevenagel adduct **I**, assisted by the synergistic interaction between the surface silanol and piperidine sites of BIL@MNP. On the other hand, the β-ketoester reacts with ammonium acetate to afford the enamine intermediate **II** in the presence of BIL@MNP as well. Then, the Michael addition reaction between these two intermediates generates the intermediate **III**, which is also promoted by BIL@MNP. Finally, the target products are formed *via* an intramolecular cyclization and elimination of H_2O.

Table 2 The one-pot four-component synthesis of polyhydroquinolines by BIL@MNP

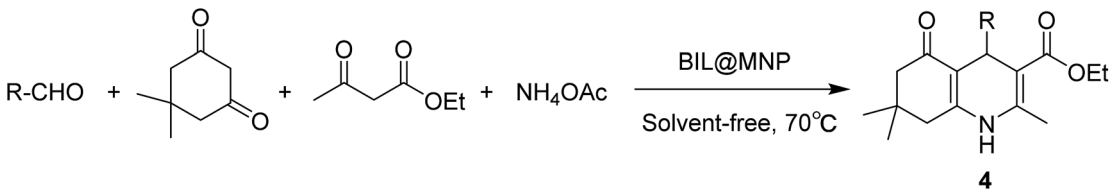

4

Entry	R	Time (min)	Product	Yield[a] (%)	Mp (°C) [Lit][ref]
1	Ph	15	**4a**	92	202–204 [203–204][29]
2	4-Me-C_6H_4	18	**4b**	90	259–261 [261–262][29]
3	4-MeO-C_6H_4	20	**4c**	91	254–256 [255–257][45]
4	4-OH-C_6H_4	30	**4d**	87	232–233 [230–231][29]
5	4-OH-3-MeO-C_6H_3	35	**4e**	93	210–211 [211–212][29]
6	3-NO_2-C_6H_4	25	**4f**	84	173–175 [174–177][35]
7	4-NO_2-C_6H_4	20	**4g**	89	241–243 [242–243][45]
8	4-F-C_6H_4	20	**4h**	85	191–193 [193–195][45]
9	4-Br-C_6H_4	15	**4i**	92	251–253 [253–255][13]
10	3-Br-C_6H_4	20	**4j**	88	232–234 [230–232][35]
11	2,4-Cl_2-C_6H_3	15	**4k**	90	244–245 [241–244][13]
12	3-Cl-C_6H_4	18	**4l**	91	203–205 [192–194][51]
13	4-Cl-C_6H_4	20	**4m**	89	243–245 [245–247][28]
14	2-Thienyl	15	**4n**	90	238–240 [238–240][13]
15	2-Furyl	18	**4o**	86	246–247 [247–248][29]
16	*n*-C_3H_7	20	**4p**	83	178–180 [165–167][52]

[a] Isolated yield.

Table 3 Catalytic activity of BIL@MNP compared with some recently reported catalysts for the one-pot four-component synthesis of **4a**

Entry	Catalyst	Conditions	Time (min)	Yield (%)	Ref.
1	$Hf(NPf_2)_4$ (1 mol%)	$C_{10}F_{18}$/60 °C	180	95	20
2	Cell-Pr-$NHSO_3H$ (50 mg)	EtOH/reflux	50	90	27
3	PdRuNi@GO (6 mg)	DMF/70 °C	45	93	31
4	Nano-Pd (4 mol%)	THF/reflux	240	89	22
5	Boehmite-SSA (30 mg)	EtOH/reflux	215	94	32
6	V–TiO_2 (2.0 mol%)	Solvent-free/80 °C	10	85	29
7	$Ni(NO_3)_2/Fe_3O_4$@SiO_2 (20 mg)	Solvent-free/100 °C	20	96	35
8	SPPN polymer (6 mg)	EtOH/120 °C/microwave	5	96	30
9	Co_3O_4-CNTs (30 mg)	EtOH/50 °C/sonication	15	97	53
10	GSA@MNPs (50 mg)	EtOH/reflux	240	90	54
11	Fe_3O_4@B-MCM-41 (50 mg)	EtOH/reflux	65	90	55
12	BIL@MNP (2.5 mol%)	Solvent-free/70 °C	15	92	This work

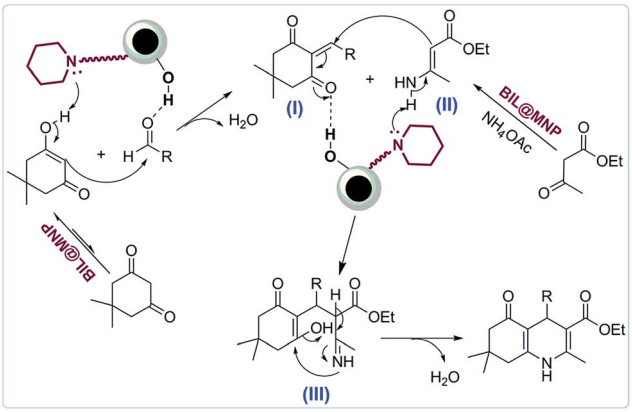

Scheme 3 Plausible mechanism for the synthesis of polyhydroquinolines.

The recovery and reuse of catalysts is highly preferable for a sustainable process. Hence, the reusability of BIL@MNP was evaluated by the reaction of benzaldehyde, dimedone, ethyl acetoacetate, and ammonium acetate under the optimized conditions. Upon completion of the reaction, ethyl acetate was added and the catalyst was simply separated by an external magnet and washed with ethyl acetate, and reused for subsequent cycles after drying under vacuum. As depicted in Fig. 6, the catalyst could be reused six times without any significant loss of catalytic activity. The recovered catalyst after six runs had no obvious change in structure, referring to the FT-IR spectra in comparison with fresh one (Fig. 7). And there was also no apparent change in the morphology and size by a TEM observation of the recovered catalyst (Fig. 3b). These results revealed that the catalyst was very stable and could endure the reaction conditions.

Moreover, a hot filtration experiment was carried out to explore the catalyst leaching. The reaction of benzaldehyde (1 mmol), dimedone (1 mmol), ethyl acetoacetate (1 mmol) and ammonium acetate (1 mmol) catalyzed by BIL@MNP (2.5 mol%) was performed at 70 °C under solvent-free conditions. When the reaction time reached 6 min, hot ethyl acetate (10 mL) was added and the BIL@MNP was fleetly separated by magnetic force. The solution was averagely divided into two sections (**S1** and **S2**). The product of **S1** was obtained in 47% yield and neat **S2** was reacted at 70 °C for another 9 min to afford the product in 49%, which was similar to **S1** and less than the normal (92%; Table 2, entry 1). Thus these above results indicated that the leaching of BIL@MNP was negligible in the catalytic process.

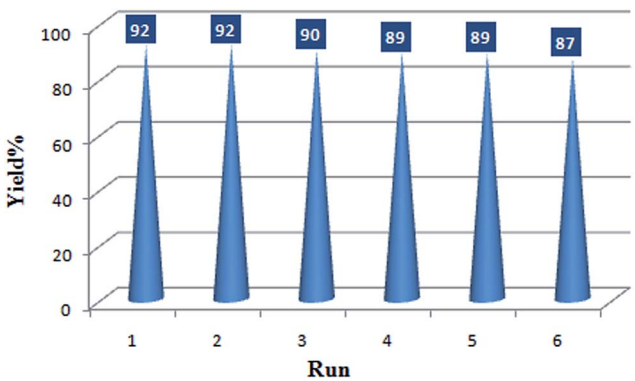

Fig. 6 Recycling experiment of BIL@MNP.

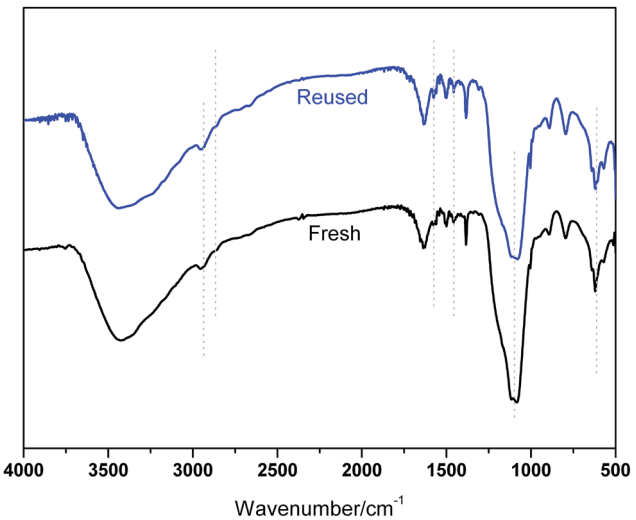

Fig. 7 FT-IR spectra of the fresh catalyst and six-times reused catalyst.

Table 4 The Knoevenagel condensation by BIL@MNP

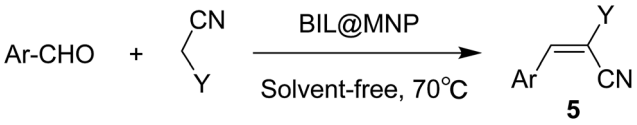

5

Entry	R	Y	Time (min)	Product	Yield (%)[a]	Mp (°C) [Lit][ref]
1	Ph	COOEt	15	**5a**	94	46–47 [47–48][56]
2	4-NO_2-C_6H_4	COOEt	12	**5b**	95	163–165 [165–167][56]
3	3-NO_2-C_6H_4	COOEt	12	**5c**	96 (96[b], 95[c], 93[d])	130–131 [130–131][57]
4	4-Cl-C_6H_4	COOEt	20	**5d**	94	87–89 [86–88][57]
5	4-F-C_6H_4	COOEt	20	**5e**	95	92–94 [90–92][56]
6	4-Br-C_6H_4	COOEt	20	**5f**	91	90–91 [88–89][58]
7	4-Me-C_6H_4	COOEt	20	**5g**	94	89–91 [89–90][59]
8	4-OH-3-MeO-C_6H_3	COOEt	35	**5h**	86	108–110 [110–111][59]
9	2-Furyl	COOEt	20	**5i**	97	86–88 [85–87][56]
10	Ph	CN	10	**5j**	97	79–80 [79–80][56]
11	3-NO_2-C_6H_4	CN	10	**5k**	95	101–102 [99–101][57]
12	4-MeO-C_6H_4	CN	20	**5l**	98	111–113 [111–113][57]

[a] Isolated yield. [b] Run 2. [c] Run 4. [d] Run 6.

Besides the synthesis of polyhydroquinolines, such an environmentally benign catalyst might provide a wider application in traditional organic base catalyzed reactions, and we additionally extended the application scope of the catalytic system to the Knoevenagel condensation. The condensation of various aldehydes and ethyl cyanoacetate or malononitrile were investigated under the above-mentioned optimized conditions. The results are summarized in Table 4. Aromatic aldehydes with electron-donating or electron-withdrawing groups, and even heteroaromatic aldehyde, underwent smoothly transformation in a short time (10–25 min) with good to excellent yields (86–98%). Moreover, the recyclability of BIL@MNP was also evaluated by the Knoevenagel condensation of 3-nitrobenzaldehyde and ethyl cyanoacetate and the yield remained almost constant in a test of six cycles (Table 4, entry 3), which shows that the BIL@MNP still had an excellent recyclability in this traditional base-catalyzed reaction.

Conclusions

In conclusion, we have developed a novel silica coated nano-Fe_3O_4 supported basic ionic liquid (BIL@MNP) as a robust and magnetically recoverable catalyst for the one-pot synthesis of polyhydroquinolines *via* the unsymmetrical Hantzsch reaction. The notable advantages of this procedure are mild reaction conditions, short reaction time, high yields and no precious metals, organic solvents or additional irradiation, which makes it a better and more practical alternative to the existing methods. Moreover, the catalyst could be simply separated by an external magnet, avoiding the tedious recovery procedure *via* filtration or centrifugation, and reused without apparent loss of activity in the test of six cycles. Besides the synthesis of polyhydroquinolines, this novel catalyst has been applied as an efficient and reusable catalyst for Knoevenagel condensation under solvent-free conditions as well and the research of application in other base-catalyzed reactions is an ongoing project.

Experimental

General

Melting points were determined on a Perkin-Elmer differential scanning calorimeter and uncorrected. ^1H and ^{13}C nuclear magnetic resonance (NMR) spectra were recorded on a Bruker AVANCE III spectrometer. The IR spectra were run on a Nicolet spectrometer (KBr). Elemental analysis was performed on Elementar Vario MICRO spectrometer. Mass spectra were obtained with an automated FININIGAN TSQ Advantage mass spectrometer. Thermogravimetric analysis was carried out under nitrogen using a Shimadzu TGA-50 spectrometer. X-Ray diffraction (XRD) images were obtained from a Bruker XRD D8 Advance instrument with Cu Kα radiation. The magnetization curve was obtained by a vibrating sample magnetometer (JDM-13T, China). Transmission electron microscope (TEM) images were obtained from a JEOL JEM-2010 instrument. All the solvents used were strictly dried according to standard operation and stored on 4A molecular sieves. All other chemicals (AR grade) were commercially available and used without further purification.

Preparation of the magnetic nanoparticle supported basic ionic liquid catalyst (BIL@MNP)

Synthesis of precursor 2 (BIL). Imidazole (7.5 g, 110 mmol) was melted at 100 °C and then NaOH (4.0 g, 100 mmol) was added with stirring for 30 min. A light yellow solid was obtained after removal of water under reduced pressure. Subsequently, 1-(2-chloroethyl)piperidine hydrochloride (9.2 g, 50 mmol) and acetonitrile (70 mL) was added. The mixture was stirred at 80 °C

for 10 h and then filtered. The filtrate was concentrated under reduced pressure, the obtained residue was dissolved in 100 mL of dichloromethane and extracted by water for several times to remove inorganic salts and excess of imidazole. After removal of solvent, 1-(2-(1*H*-imidazol-1-yl)ethyl)piperidine (**1**) was obtained as a yellow liquid in 94% yield and used for the next reaction without further purification.

^{1}H NMR (500 MHz, $CDCl_3$) δ 7.43 (s, 1H), 6.92 (s, 1H), 6.87 (s, 1H), 3.92 (q, J = 6.5 Hz, 2H), 2.52 (t, J = 6.5 Hz, 2H), 2.30 (s, 4H), 1.49–1.45 (m, 4H), 1.35–1.32 (m, 2H); ^{13}C NMR (125 MHz, $CDCl_3$) δ 137.14, 128.78, 119.09, 59.21, 54.45, 44.59, 25.80, 24.00.

3-Chloropropyltriethoxysilane (5.0 mL, 21 mmol) was added dropwise into a solution of **1** (3.6 g, 20 mmol) in acetonitrile (30 mL) under a nitrogen atmosphere and the mixture was refluxed for three days. The solvent was removed by rotatory evaporation under reduced pressure and the obtained residue was washed with absolute ether for several times, then dried under vacuum to give the precursor **2** as a viscous orange liquid in 92% yield.

^{1}H NMR (500 MHz, $CDCl_3$) δ 10.17 (s, 1H), 7.64 (s, 1H), 7.28 (s, 1H), 4.33 (t, J = 5.5 Hz, 2H), 4.17 (t, J = 7.5 Hz, 2H), 3.64 (q, J = 7.0 Hz, 6H), 2.58 (t, J = 5.5 Hz, 2H), 2.27 (s, 1H), 1.87–1.81 (m, 2H), 1.38–1.34 (m, 4H), 1.25 (s, 2H), 1.04 (t, J = 7.0 Hz, 9H), 0.44 (t, J = 8.0 Hz, 2H); ^{13}C NMR (125 MHz, $CDCl_3$) δ 137.26, 122.98, 121.18, 58.41, 57.71, 54.20, 51.51, 46.68, 25.84, 24.25, 23.93, 18.12, 6.97; FT-IR (KBr, cm^{-1}): 3146, 3093, 2986, 2941, 2866, 2809, 1645, 1563, 1456, 1394, 1355, 1172, 1085, 959, 782, 650; ESI-MS: m/z 384.2 (M^+–Cl); anal. calc. for $C_{19}H_{38}ClN_3O_3Si$: C, 54.33; H, 9.12; N, 10.00. Found: C, 54.49; H, 9.71; N, 9.89.

Synthesis of silica-coated Fe_3O_4 nanoparticle (SiO_2@Fe_3O_4). The core–shell SiO_2@Fe_3O_4 nanoparticles were prepared by a modified Stöber method in our previous work.[46]

Procedure for the synthesis of BIL@MNP. 1.0 g of SiO_2@Fe_3O_4 nanoparticles were dispersed in 50 mL of chloroform by sonication. A chloroform solution of precursor **2** (1.0 g/50 mL) was then added, and the mixture was refluxed for two days under nitrogen. After being cooled to room temperature, the target product BIL@MNP was collected by a permanent magnet and rinsed thrice with chloroform (30 mL), and then dried under vacuum overnight.

General procedure for the synthesis of polyhydroquinolines

A mixture of aldehyde (1 mmol), dimedone (1 mmol), ethyl acetoacetate (1 mmol), ammonium acetate (1 mmol) and BIL@MNP (70 mg) was stirred at 70 °C in an oil bath for a certain time, as indicated by TLC for a complete reaction. Ethyl acetate was added and the catalyst was separated magnetically from the product solution, washed with ethyl acetate, and dried under vacuum. Pure polyhydroquinolines were afforded by evaporation of the solvent followed by recrystallization from the ethanol–water mixture. All products were characterized by spectral data and compared with their physical data given in the literature.

Ethyl 2,7,7-trimethyl-5-oxo-4-phenyl-1,4,5,6,7,8-hexahydroquinoline-3-carboxylate (4a). Melting point: 202–204 °C; FT-IR (KBr, cm^{-1}): 3290, 3220, 3082, 2964, 2932, 1699, 1611, 1484, 1382, 1280, 1212, 1072, 760, 698, 530; ^{1}H NMR (500 MHz, $CDCl_3$) δ 7.51 (s, 1H), 7.32 (t, J = 7.5 Hz, 2H), 7.20 (t, J = 7.5 Hz, 2H), 7.10 (t, J = 7.5 Hz, 1H), 5.07 (s, 1H), 4.08 (q, J = 7.0, 2H), 2.31 (s, 3H), 2.26–2.16 (m, 4H), 1.22 (t, J = 7.0 Hz, 3H), 1.05 (s, 3H), 0.93 (s, 3H).

Ethyl 2,7,7-trimethyl-5-oxo-4-(*p*-tolyl)-1,4,5,6,7,8-hexahydroquinoline-3-carboxylate (4b). Melting point: 259–261 °C; FT-IR (KBr, cm^{-1}): 3276, 3208, 3079, 2959, 1702, 1606, 1492, 1381, 1282, 1216, 1072, 848, 531; ^{1}H NMR (400 MHz, $CDCl_3$) δ 7.18 (d, J = 7.9 Hz, 2H), 6.99 (d, J = 7.8 Hz, 2H), 6.45–6.20 (m, 1H), 5.01 (s, 1H), 4.06 (q, J = 7.1 Hz, 2H), 2.33 (s, 3H), 2.30–2.28 (m, 1H), 2.24 (s, 3H), 2.23–2.11 (m, 3H), 1.21 (t, J = 7.1 Hz, 3H), 1.06 (s, 3H), 0.94 (s, 3H).

Ethyl 4-(4-methoxyphenyl)-2,7,7-trimethyl-5-oxo-1,4,5,6,7,8-hexahydroquinoline-3-carboxylate (4c). Melting point: 254–256 °C; FT-IR (KBr, cm^{-1}): 3277, 3209, 3079, 2958, 1702, 1606, 1498, 1380, 1281, 1215, 1072, 850, 536; ^{1}H NMR (400 MHz, $CDCl_3$) δ 7.21 (d, J = 6.6 Hz, 2H), 6.73 (d, J = 6.4 Hz, 2H), 6.64–6.33 (m, 1H), 5.00 (s, 1H), 4.07 (d, J = 6.0 Hz, 2H), 3.72 (s, 3H), 2.34 (s, 3H), 2.25–2.12 (m, 4H), 1.21 (s, 3H), 1.05 (s, 3H), 0.93 (s, 3H).

Ethyl 4-(4-hydroxyphenyl)-2,7,7-trimethyl-5-oxo-1,4,5,6,7,8-hexahydroquinoline-3-carboxylate (4d). Melting point: 232–233 °C; ^{1}H NMR (500 MHz, DMSO-d_6) δ 9.03 (s, 1H), 8.96 (s, 1H), 6.93 (d, J = 8.4 Hz, 2H), 6.56 (d, J = 8.4 Hz, 2H), 4.74 (s, 1H), 3.99–3.95 (m, 2H), 2.40 (d, J = 17.0 Hz, 1H), 2.28 (d, J = 11.3 Hz, 4H), 2.15 (d, J = 16.1 Hz, 1H), 1.97 (d, J = 16.1 Hz, 1H), 1.14 (t, J = 7.1 Hz, 3H), 1.01 (s, 3H), 0.86 (s, 3H).

Ethyl 4-(4-hydroxy-3-methoxyphenyl)-2,7,7-trimethyl-5-oxo-1,4,5,6,7,8-hexahydroquinoline-3-carboxylate (4e). Melting point: 210–211 °C; FT-IR (KBr, cm^{-1}): 3399, 2393, 3067, 2951, 1698, 1590, 1482, 1380, 1270, 1216, 1069, 784, 725, 521; ^{1}H NMR (400 MHz, $CDCl_3$) δ 6.93 (d, J = 1.7 Hz, 1H), 6.71 (dt, J = 8.2, 5.0 Hz, 2H), 5.70 (s, 1H), 5.42 (s, 1H), 4.98 (s, 1H), 4.07 (q, J = 7.1 Hz, 2H), 3.85 (s, 3H), 2.38 (s, 3H), 2.36–2.14 (m, 4H), 1.21 (t, J = 7.1 Hz, 3H), 1.08 (s, 3H), 0.95 (s, 3H).

Ethyl 2,7,7-trimethyl-4-(3-nitrophenyl)-5-oxo-1,4,5,6,7,8-hexahydroquinoline-3-carboxylate (4f). Melting point: 173–175 °C; FT-IR (KBr, cm^{-1}): 3283, 3212, 3076, 2959, 1705, 1607, 1533, 1487, 1380, 1353, 1281, 1211, 1072, 807, 721, 682, 526; ^{1}H NMR (400 MHz, $CDCl_3$) δ 8.11 (t, J = 1.8 Hz, 1H), 8.02–7.94 (m, 1H), 7.73 (d, J = 7.7 Hz, 1H), 7.37 (t, J = 7.9 Hz, 1H), 6.39 (d, J = 6.6 Hz, 1H), 5.16 (s, 1H), 4.07 (q, J = 7.1 Hz, 2H), 2.42–2.11 (m, 7H), 1.20 (t, J = 7.1 Hz, 3H), 1.09 (s, 3H), 0.93 (s, 3H).

Ethyl 2,7,7-trimethyl-4-(4-nitrophenyl)-5-oxo-1,4,5,6,7,8-hexahydroquinoline-3-carboxylate (4g). Melting point: 241–243 °C; ^{1}H NMR (500 MHz, $CDCl_3$) δ 8.01 (d, J = 8.7 Hz, 2H), 7.42 (d, J = 8.7 Hz, 2H), 6.27 (s, 1H), 5.09 (s, 1H), 3.98 (q, J = 7.1 Hz, 2H), 2.33–2.89 (m, 4H), 2.17 (d, J = 16.4 Hz, 2H), 2.07 (d, J = 16.3 Hz, 1H), 1.11 (t, J = 7.1 Hz, 3H), 1.01 (s, 3H), 0.83 (s, 3H).

Ethyl 4-(4-fluorophenyl)-2,7,7-trimethyl-5-oxo-1,4,5,6,7,8-hexahydroquinoline-3-carboxylate (4h). Melting point: 191–193 °C; ^{1}H NMR (300 MHz, $CDCl_3$) δ 7.21–7.16 (m, 2H), 6.81 (ddd, J = 8.8, 5.9, 2.5 Hz, 2H), 5.72 (s, 1H), 4.96 (s, 1H), 3.98 (q, J = 7.1 Hz, 2H), 2.37–2.04 (m, 7H), 1.12 (t, J = 7.1 Hz, 3H), 1.01 (s, 3H), 0.86 (s, 3H).

Ethyl 4-(4-bromophenyl)-2,7,7-trimethyl-5-oxo-1,4,5,6,7,8-hexahydroquinoline-3-carboxylate (4i). Melting point: 251–253 °C; ^{1}H NMR (300 MHz, $CDCl_3$) δ 7.35–7.28 (m, 2H), 7.24–7.13 (m, 2H), 5.70 (s, 1H), 5.01 (s, 1H), 4.05 (q, J = 7.1 Hz, 2H), 2.46–2.08 (m, 7H), 1.19 (t, J = 7.1 Hz, 3H), 1.08 (s, 3H), 0.93 (s, 3H).

Ethyl 4-(3-bromophenyl)-2,7,7-trimethyl-5-oxo-1,4,5,6,7,8-hexahydroquinoline-3-carboxylate (4j). Melting point: 232–234 °C; ^{1}H NMR (500 MHz, $CDCl_3$) δ 7.43 (s, 1H), 7.27 (d, J = 8.1 Hz, 1H), 7.24 (d, J = 8.0 Hz, 1H), 7.08 (t, J = 7.8 Hz, 1H), 6.77 (s, 1H), 5.03 (s, 1H), 4.09–4.05 (m, 2H), 2.35 (s, 3H), 2.30–2.15 (m, 4H), 1.23 (t, J = 7.1 Hz, 3H), 1.08 (s, 3H), 0.96 (s, 3H).

Ethyl 4-(2,4-dichlorophenyl)-2,7,7-trimethyl-5-oxo-1,4,5,6,7,8-hexahydroquinoline-3-carboxylate (4k). Melting point: 240–242 °C; ^{1}H NMR (300 MHz, $CDCl_3$) δ 7.33 (d, J = 8.4 Hz, 1H), 7.26 (s, 1H), 7.10 (dd, J = 8.3, 2.2 Hz, 1H), 5.79 (s, 1H), 5.33 (s, 1H), 4.12–3.96 (m, 2H), 2.39–2.12 (m, 7H), 1.18 (t, J = 7.1 Hz, 3H), 1.08 (s, 3H), 0.95 (s, 3H).

Ethyl 4-(3-chlorophenyl)-2,7,7-trimethyl-5-oxo-1,4,5,6,7,8-hexahydroquinoline-3-carboxylate (4l). Melting point: 203–205 °C; ^{1}H NMR (500 MHz, $CDCl_3$) δ 7.19 (t, J = 1.8 Hz, 1H), 7.15 (d, J = 7.6 Hz, 1H), 7.06 (t, J = 7.7 Hz, 1H), 7.03–6.99 (m, 1H), 6.51–6.49 (m, 1H), 4.97 (s, 1H), 4.07–3.94 (m, 2H), 2.29 (s, 3H), 2.25 (d, J = 16.7 Hz, 1H), 2.16 (dd, J = 16.6, 6.2 Hz, 2H), 2.09 (d, J = 16.3 Hz, 1H), 1.14 (t, J = 7.1 Hz, 3H), 1.00 (s, 3H), 0.88 (s, 3H).

Ethyl 4-(4-chlorophenyl)-2,7,7-trimethyl-5-oxo-1,4,5,6,7,8-hexahydroquinoline-3-carboxylate (4m). Melting point: 243–245 °C; ^{1}H NMR (300 MHz, $CDCl_3$) δ 7.26–7.20 (m, 2H), 7.20–7.12 (m, 2H), 5.93 (s, 1H), 5.02 (s, 1H), 4.05 (q, J = 7.1 Hz, 2H), 2.42–2.09 (m, 7H), 1.19 (t, J = 7.1 Hz, 3H), 1.08 (s, 3H), 0.93 (s, 3H).

Ethyl 2,7,7-trimethyl-5-oxo-4-(thiophen-2-yl)-1,4,5,6,7,8-hexahydroquinoline-3-carboxylate (4n). Melting point: 238–240 °C; ^{1}H NMR (300 MHz, DMSO) δ 9.24 (s, 1H), 7.17 (dd, J = 5.1, 1.2 Hz, 1H), 6.82 (dd, J = 5.1, 3.5 Hz, 1H), 6.70–6.61 (m, 1H), 5.16 (s, 1H), 4.06 (q, J = 7.1 Hz, 2H), 2.46–2.00 (m, 7H), 1.19 (t, J = 7.1 Hz, 3H), 1.02 (s, 3H), 0.94 (s, 3H).

Ethyl 4-(furan-2-yl)-2,7,7-trimethyl-5-oxo-1,4,5,6,7,8-hexahydroquinoline-3-carboxylate (4o). Melting point: 246–247 °C; ^{1}H NMR (300 MHz, DMSO) δ 9.16 (s, 1H), 7.36 (dd, J = 1.8, 0.9 Hz, 1H), 6.23 (dd, J = 3.1, 1.8 Hz, 1H), 5.83 (d, J = 3.1 Hz, 1H), 5.02 (s, 1H), 4.14–3.96 (m, 2H), 2.45–1.97 (m, 7H), 1.18 (t, J = 7.1 Hz, 3H), 1.02 (s, 3H), 0.93 (s, 3H).

Ethyl 2,7,7-trimethyl-5-oxo-4-propyl-1,4,5,6,7,8-hexahydroquinoline-3-carboxylate (4p). Melting point: 178–180 °C; ^{1}H NMR (300 MHz, $CDCl_3$) δ 5.64 (s, 1H), 4.24–4.09 (m, 2H), 4.02 (t, J = 5.3 Hz, 1H), 2.41–2.05 (m, 7H), 1.39–1.18 (m, 7H), 1.09 (s, 6H), 0.83 (t, J = 7.1 Hz, 3H).

General procedure for Knoevenagel condensation

A mixture of aromatic aldehyde (1 mmol), activated methylene compounds (1.1 mmol), and BIL@MNP (70 mg) was stirred at 70 °C in an oil bath for a certain time, as indicated by TLC for a complete reaction. Ethyl acetate was added and the catalyst was separated magnetically from the product solution, washed with ethyl acetate, and dried under vacuum. The pure final products were afforded by evaporation of the solvent followed by recrystallization from the ethanol-water mixture. All products were characterized by spectral data and compared with their physical data given in the literature.

Selected data for typical compounds

Ethyl (*E*)-2-cyano-3-phenylacrylate (5a). Melting point: 46–47 °C; FT-IR (KBr, cm^{-1}): 3031, 2981, 2224, 1727, 1608, 1447, 1259, 1203, 1090, 768, 684; ^{1}H NMR (400 MHz, $CDCl_3$) δ 8.28 (s, 1H), 8.01 (dd, J = 5.3, 3.5 Hz, 2H), 7.62–7.48 (m, 3H), 4.42 (q, J = 7.1 Hz, 2H), 1.43 (t, J = 7.1 Hz, 3H).

Ethyl (*E*)-2-cyano-3-(4-nitrophenyl)acrylate (5b). ^{1}H NMR (300 MHz, $CDCl_3$) δ 8.32–8.26 (m, 2H), 8.24 (s, 1H), 8.10–8.04 (m, 2H), 4.36 (q, J = 7.1 Hz, 2H), 1.36 (t, J = 7.1 Hz, 3H).

Ethyl (*E*)-2-cyano-3-(3-nitrophenyl)acrylate (5c). Melting point: 130–131 °C; FT-IR (KBr, cm^{-1}): 3071, 2989, 2227, 1720, 1606, 1530, 1356, 1268, 1207, 1097, 812, 765, 671; ^{1}H NMR (400 MHz, $CDCl_3$) δ 8.72 (s, 1H), 8.43 (dd, J = 9.8, 4.4 Hz, 2H), 8.33 (s, 1H), 7.76 (t, J = 8.1 Hz, 1H), 4.45 (q, J = 7.1 Hz, 2H), 1.44 (t, J = 7.1 Hz, 3H).

Ethyl (*E*)-3-(4-chlorophenyl)-2-cyanoacrylate (5d). ^{1}H NMR (300 MHz, $CDCl_3$) δ 8.13 (s, 1H), 7.92–7.82 (m, 2H), 7.49–7.35 (m, 2H), 4.32 (q, J = 7.1 Hz, 2H), 1.33 (t, J = 7.1 Hz, 3H).

Ethyl (*E*)-2-cyano-3-(4-fluorophenyl)acrylate (5e). Melting point: 92–94 °C; FT-IR (KBr, cm^{-1}): 3038, 2996, 2227, 1719, 1595, 1510, 1203, 1088, 843; ^{1}H NMR (400 MHz, $CDCl_3$) δ 8.23 (s, 1H), 8.10–8.00 (m, 2H), 7.27–7.16 (m, 2H), 4.41 (q, J = 7.1 Hz, 2H), 1.42 (t, J = 7.1 Hz, 3H).

Ethyl (*E*)-3-(4-bromophenyl)-2-cyanoacrylate (5f). ^{1}H NMR (300 MHz, $CDCl_3$) δ 8.12 (s, 1H), 7.78 (t, J = 5.4 Hz, 2H), 7.62–7.54 (m, 2H), 4.32 (q, J = 7.1 Hz, 2H), 1.33 (t, J = 7.1 Hz, 3H).

Ethyl (*E*)-2-cyano-3-(*p*-tolyl)acrylate (5g). Melting point: 89–91 °C; FT-IR (KBr, cm^{-1}): 3029, 2992, 2217, 1725, 1596, 1272, 1191, 1094, 816; ^{1}H NMR (400 MHz, $CDCl_3$) δ 8.24 (s, 1H), 7.92 (d, J = 8.2 Hz, 2H), 7.33 (d, J = 8.1 Hz, 2H), 4.40 (q, J = 7.1 Hz, 2H), 2.46 (s, 3H), 1.42 (t, J = 7.1 Hz, 3H).

Ethyl (*E*)-2-cyano-3-(4-hydroxy-3-methoxyphenyl)acrylate (5h). Melting point: 108–110 °C; FT-IR (KBr, cm^{-1}): 3273, 2982, 2942, 2229, 1721, 1577, 1510, 1276, 1217, 1096, 855; ^{1}H NMR (400 MHz, $CDCl_3$) δ 8.16 (s, 1H), 7.87 (d, J = 2.0 Hz, 1H), 7.41 (dd, J = 8.3, 2.0 Hz, 1H), 7.02 (d, J = 8.3 Hz, 1H), 6.30 (s, 1H), 4.39 (q, J = 7.1 Hz, 2H), 4.00 (s, 3H), 1.41 (t, J = 7.1 Hz, 3H).

Ethyl (*E*)-2-cyano-3-(furan-2-yl)acrylate (5i). Melting point: 86–88 °C; FT-IR (KBr, cm^{-1}): 3040, 2926, 2224, 1716, 1621, 1262, 1212, 1025, 761; ^{1}H NMR (400 MHz, $CDCl_3$) δ 8.04 (s, 1H), 7.77 (d, J = 1.4 Hz, 1H), 7.42 (d, J = 3.6 Hz, 1H), 6.68 (dd, J = 3.6, 1.6 Hz, 1H), 4.38 (q, J = 7.1 Hz, 2H), 1.40 (t, J = 7.1 Hz, 3H).

2-Benzylidenemalononitrile (5j). Melting point: 79–80 °C; FT-IR (KBr, cm^{-1}): 3033, 2985, 2223, 1591, 1568, 1450, 1218, 1157, 958, 755; ^{1}H NMR (300 MHz, $CDCl_3$) δ 7.90–7.81 (m, 2H), 7.72 (s, 1H), 7.61–7.54 (m, 1H), 7.48 (t, J = 7.5 Hz, 2H).

2-(3-Nitrobenzylidene)malononitrile (5k). Melting point: 101–102 °C; ^{1}H NMR (300 MHz, $CDCl_3$) δ 8.59 (t, J = 1.9 Hz, 1H), 8.41 (ddd, J = 8.3, 2.1, 0.9 Hz, 1H), 8.27 (d, J = 7.9 Hz, 1H), 7.83 (s, 1H), 7.73 (t, J = 8.1 Hz, 1H).

2-(4-Methoxybenzylidene)malononitrile (5l). Melting point: 111–113 °C; FT-IR (KBr, cm^{-1}): 3029, 2985, 2223, 1606, 1571, 1513, 1279, 1184, 1022, 833; ^1H NMR (400 MHz, $CDCl_3$) δ 7.93 (d, $J = 8.8$ Hz, 2H), 7.67 (s, 1H), 7.04 (d, $J = 8.8$ Hz, 2H), 3.94 (s, 3H).

Conflicts of interest

There are no conflicts to declare.

Acknowledgements

The work is financially supported by Natural Science Foundation of Jiangsu Province (China) (No. BK20150282); Innovation and Entrepreneurship Training Program for Undergraduates in Jiangsu Province (201713985010Y, 201710332051X); A project funded by the Priority Academic Program Development (PAPD) of Jiangsu Higher Education Institutions. The authors would like to thank Excellent Innovation Team in Science and Technology of Education Department of Jiangsu Province for discussions.

References

1 J. P. Wan and Y. Liu, *RSC Adv.*, 2012, **2**, 9763–9777.
2 V. K. Sharma and S. K. Singh, *RSC Adv.*, 2017, **7**, 2682–2732.
3 K. C. Yedinak, *Am. Pharm.*, 1993, **33**, 49–64.
4 M. Kawase, A. Shah, H. Gaveriya, N. Motohashi, H. Sakagami, A. Varga and J. Molnár, *Bioorg. Med. Chem.*, 2002, **10**, 1051–1055.
5 P. S. Eharkar, B. Desai, H. Gaveria, B. Varu, R. Loriya, Y. Naliapara, A. Shah and V. M. Kulkarni, *J. Med. Chem.*, 2002, **45**, 4858–4867.
6 A. K. Ogawa, C. A. Willoughby, R. Bergeron, K. P. Ellsworth, W. M. Geissler, R. W. Myer, J. Yao, H. Harris and K. T. Chapman, *Bioorg. Med. Chem. Lett.*, 2003, **13**, 3405–3408.
7 K. Sirisha, D. Bikshapathi, G. Achaiah and V. M. Reddy, *Eur. J. Med. Chem.*, 2011, **46**, 1564–1571.
8 P. A. Hopes, A. J. Parker and I. Patel, *Org. Process Res. Dev.*, 2006, **10**, 808–813.
9 J. Marco-Contelles, R. León, C. de los Rios, A. Guglietta, J. Terencio, M. G. López, A. G. Garcia and M. Villarroya, *J. Med. Chem.*, 2006, **49**, 7607–7610.
10 R. León, C. de los Rios, J. Marco-Contelles, O. Huertas, X. Barril, F. J. Luque, M. G. López, A. G. García and M. Villarroya, *Bioorg. Med. Chem.*, 2008, **16**, 7759–7769.
11 C. Zheng and S. L. You, *Chem. Soc. Rev.*, 2012, **41**, 2498–2518.
12 A. Hantzsch, *Ber. Dtsch. Chem. Ges.*, 1881, **14**, 1637–1638.
13 L. M. Wang, J. Sheng, L. Zhang, J. W. Han, Z. Y. Fan, H. Tian and C. T. Qian, *Tetrahedron*, 2005, **61**, 1539–1543.
14 J. L. Donelson, R. A. Gibbs and S. K. De, *J. Mol. Catal. A: Chem.*, 2006, **256**, 309–311.
15 A. Kumar and R. A. Maurya, *Tetrahedron*, 2007, **63**, 1946–1952.
16 A. Kumar and R. A. Maurya, *Tetrahedron Lett.*, 2007, **48**, 3887–3890.
17 S. K. Ko and C. F. Yao, *Tetrahedron*, 2006, **62**, 7293–7299.
18 A. Kumar and R. A. Maurya, *Synlett*, 2008, 883–885.
19 R. Surasani, D. Kalita, A. V. D. Rao, K. Yarbagi and K. B. Chandrasekhar, *J. Fluorine Chem.*, 2012, **135**, 91–96.
20 M. Hong, C. Cai and W. B. Yi, *J. Fluorine Chem.*, 2010, **131**, 111–114.
21 S. B. Sapkal, K. F. Shelke, B. B. Shingate and M. S. Shingare, *Tetrahedron Lett.*, 2009, **50**, 1754–1756.
22 M. Saha and A. K. Pal, *Tetrahedron Lett.*, 2011, **52**, 4872–4877.
23 S. J. Yü, S. Wu, X. M. Zhao and C. W. Lü, *Res. Chem. Intermed.*, 2017, **43**, 3121–3130.
24 B. D. Bala, K. Balamurugan and S. Perumal, *Tetrahedron Lett.*, 2011, **52**, 4562–4566.
25 S. Guo and Y. Yuan, *Chin. J. Chem.*, 2010, **28**, 811–817.
26 R. F. Affeldt, E. V. Benvenutti and D. Russowsky, *New J. Chem.*, 2012, **36**, 1502–1511.
27 S. Karhale, C. Bhenki, G. Rashinkar and V. Helavi, *New J. Chem.*, 2017, **41**, 5133–5141.
28 D. Elhamifar, P. Badin and G. Karimipoor, *J. Colloid Interface Sci.*, 2017, **499**, 120–127.
29 G. B. Dharma Rao, S. Nagakalyan and G. K. Prasad, *RSC Adv.*, 2017, **7**, 3611–3616.
30 S. Mondal, B. C. Patra and A. Bhaumik, *ChemCatChem*, 2017, **9**, 1469–1475.
31 T. Demirci, B. Çelik, Y. Yıldız, S. Eriş, M. Arslan, F. Sen and B. Kilbas, *RSC Adv.*, 2016, **6**, 76948–76956.
32 A. Ghorbani-Choghamarani and B. Tahmasbi, *New J. Chem.*, 2016, **40**, 1205–1212.
33 A. Amoozadeh, S. Rahmani, M. Bitaraf, F. B. Abadi and E. Tabrizian, *New J. Chem.*, 2016, **40**, 770–780.
34 L. Shiri, A. Ghorbani-Choghamarani and M. Kazemi, *Monatsh. Chem.*, 2017, **148**, 1131–1139.
35 L. Shiri, L. Heidari and M. Kazemi, *Appl. Organomet. Chem.*, 2017, e3943.
36 J. P. Hallett and T. Welton, *Chem. Rev.*, 2011, **111**, 3508–3576.
37 C. Dai, J. Zhang, C. Huang and Z. Lei, *Chem. Rev.*, 2017, **117**, 6929–6983.
38 S. G. Zhang, J. H. Zhang, Y. Zhang and Y. Q. Deng, *Chem. Rev.*, 2017, **117**, 6755–6833.
39 D. Wang and D. Astruc, *Chem. Rev.*, 2014, **114**, 6949–6985.
40 R. B. N. Baig, M. N. Nadagouda and R. S. Varma, *Coord. Chem. Rev.*, 2015, **287**, 137–156.
41 M. B. Gawande, Y. Monga, R. Zboril and R. K. Sharma, *Coord. Chem. Rev.*, 2015, **288**, 118–143.
42 A. K. Rathi, M. B. Gawande, J. Pechousek, C. Aparicio, M. Petr, K. Cepe, R. Krikavova, Z. Travnicek and R. Zboril, *Green Chem.*, 2016, **18**, 2363–2373.
43 H. N. Dadhania, D. K. Raval and A. N. Dadhania, *Catal. Sci. Technol.*, 2015, **5**, 4806–4812.
44 N. Candu, C. Rizescu, I. Podolean, M. Tudorache, V. I. Parvulescu and S. M. Coman, *Catal. Sci. Technol.*, 2015, **5**, 729–737.
45 M. Yarie, M. A. Zolfigol, Y. Bayat, A. Asgari, D. A. Alonso and A. Khoshnood, *RSC Adv.*, 2016, **6**, 82842–82853.
46 Q. Zhang, H. Su, J. Luo and Y. Y. Wei, *Green Chem.*, 2012, **14**, 201–208.

47 Q. Zhang, H. Su, J. Luo and Y. Y. Wei, *Tetrahedron*, 2013, **69**, 447–454.
48 Q. Zhang, H. Su, J. Luo and Y. Y. Wei, *Catal. Sci. Technol.*, 2013, **3**, 235–243.
49 Q. Zhou, Z. Wan, X. Yuan and J. Luo, *Appl. Organomet. Chem.*, 2016, **30**, 215–220.
50 Q. Zhang, X. Zhao, H. X. Wei, J. H. Li and J. Luo, *Appl. Organomet. Chem.*, 2017, **31**, e3608.
51 B. L. Li, A. G. Zhong and A. G. Ying, *J. Heterocycl. Chem.*, 2015, **52**, 445–449.
52 A. Davoodnia, M. Khashi and N. Tavakoli-Hoseini, *Chin. J. Catal.*, 2013, **34**, 1173–1178.
53 Z. Zarnegar, J. Safari and Z. M. Kafroudi, *New J. Chem.*, 2015, **39**, 1445–1451.
54 M. Hajjami and B. Tahmasbi, *RSC Adv.*, 2015, **5**, 59194–59203.
55 M. Abdollahi-Alibeik and A. Rezaeipoor-Anari, *J. Magn. Magn. Mater.*, 2016, **398**, 205–214.
56 G. W. Li, J. Xiao and W. Q. Zhang, *Green Chem.*, 2012, **14**, 2234–2242.
57 R. Khoshnavazi, L. Bahrami and F. Havasi, *RSC Adv.*, 2016, **6**, 100962–100975.
58 D. Khan, S. Mukhtar, M. A. Alsharif, M. I. Alahmdi and N. Ahmed, *Tetrahedron Lett.*, 2017, **58**, 3183–3187.
59 H. Kiyani and F. Ghorbani, *Res. Chem. Intermed.*, 2015, **41**, 7847–7882.